

Columnar Mesomorphism of Bi- and Trinuclear Ni(II), Cu(II), and VO(II) *cis*-Enaminoketone Complexes with Low Symmetry

Jadwiga Szydłowska,* Adam Krówczyński, Ewa Górecka, and Damian Pocięcha

Chemistry Department, Warsaw University, Laboratory of Dielectrics and Magnetics,
Al. Zwirki i Wigury 101, 02-089 Warsaw, Poland

Received January 25, 2000

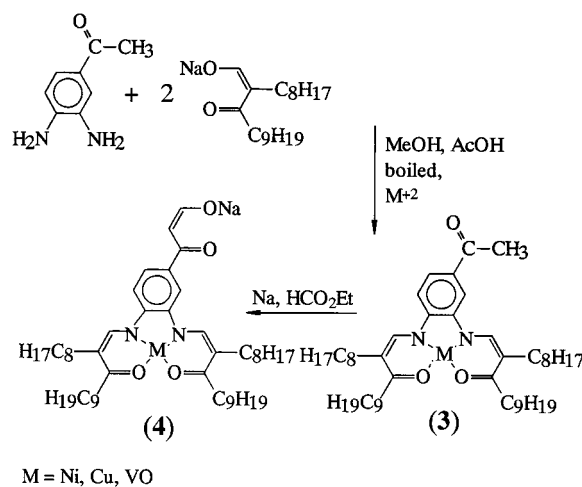
New enaminoketone tetradentate bi- and trinuclear complexes creating columnar mesophases are reported. Various combinations of nickel, copper, or vanadyl ions were applied as metallic centers. Because of the bowl-like structure of chelating centers and the low molecular symmetry (C_s) the bivanadyl complexes form two diastereoisomers, which were separated. The superexchange coupling of the electron spins of paramagnetic centers copper–copper and vanadyl–vanadyl was found for binuclear complexes in ESR studies.

1. Introduction

Molecular shape serves as a dominant factor in determining the organization of molecules into a liquid crystalline phase. It is well-known that flat or pyramidal molecules organize easily into columns and that numerous noncovalent interactions such as van der Waals or π -stacking play an important role in forming a molecular assembly. There are also some suggestions that ligand–metal or metal–metal weak bondings promote the appearance of the columnar phases.^{1–3} Here we present detailed studies of the columnar organization of metallomesogenic flat or pyramidal-shaped molecules containing two or three different metal ions. Intermolecular as well as intramolecular interactions were studied for these compounds.

We designed and synthesized new multinuclear *cis*-enaminoketone complexes. As ligands, the enaminoketone moieties were used because they offer an opportunity to form chemically stable complexes with shapes that can be readily modified.^{4–8} Compounds **1** and **2** consisting of two and three nuclear centers, respectively, were formed from two or three tetradentate chelating moieties joined together by single bonds. As the metallic centers, the nickel, copper, and vanadyl ions were applied. The binuclear complexes **1** with nickel or copper ions reveal C_s molecular symmetry, whereas the oxovanadium metallic centers lower this symmetry to C_1 . The designed structures of three metallic compounds of **2** for nickel or copper ions have C_{2v} symmetry. Insertion of the vanadyl center into position between the other metallic ions results in C_s symmetry.

Scheme 1



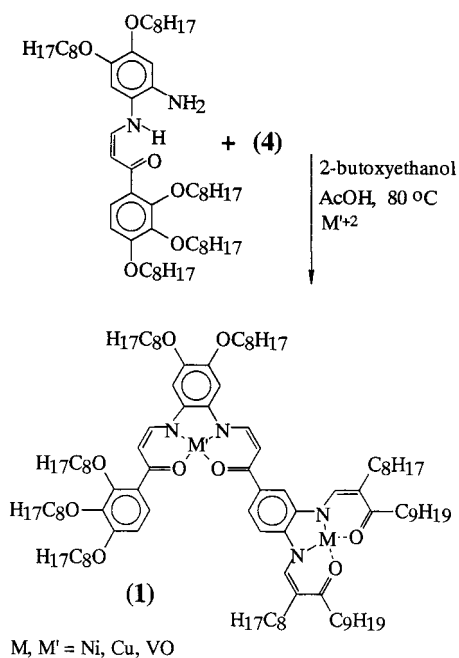
2. Experimental Section

2.1. Synthesis. Synthetic procedures to obtain the series of complexes **1** and **2** are sketched in Schemes 1–3. In the first common step (Scheme 1) the reaction chain gives a mononuclear *cis*-enaminoketone complex (**4**), which is further attached to the mono- or diamino compound (Schemes 2 and 3), that results in complexes with two or three metallic centers (**1** or **2**, respectively). Results from the elemental and NMR analyses of the synthesized nickel complexes are consistent with the expected structure without any sign of additives or impurities. Infrared spectra were recorded on a spectrometer in chloromethylene solution, and UV–vis spectra were recorded in the same solvent on a Shimadzu UV-3101 PC scanning spectrometer. Mass spectra were taken from a Mariner PerSeptive Biosystem mass spectrometer (electron spray mode) and are consistent with the assumed molecular structure.

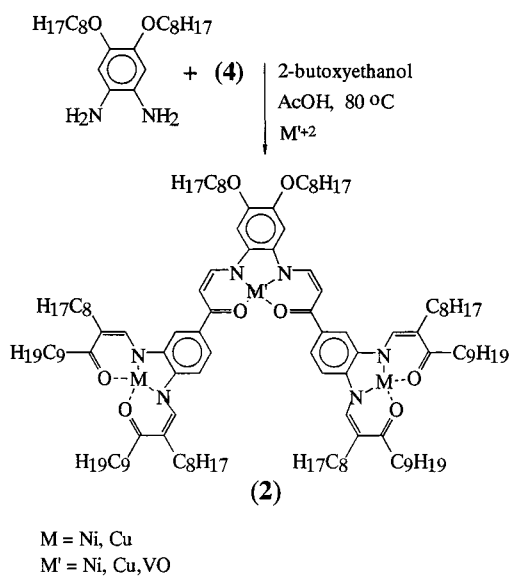
2.1.1. [1,2-Di(2'-octyl-3'-oxo-1'-dodecenyldiamino)-4-acetylbenzene]metal(II) (3). The sodium salt of formyl ketone (2.2 mmol) (obtained from 9-nonadecanone) and 3,4-diaminoacetophenone (1 mmol) were dissolved in ethanol (150 cm³), neutralized with acetic acid (to pH about 6), and boiled for 10 min. To the boiling mixture an appropriate salt of the metal, 1 mmol of Ni(OAc)₂, Cu(OAc)₂, or VO(acac)₂ was added. After 5 min of reflux the mixture was cooled, resulting in a precipitate (**3**) that was filtered off and recrystallized from hexane. The vanadyl complex, which was released as a green, thick oil, was decanted several times with methanol. The remnants of methanol in the oil were

- (1) Abied, H.; Gulion, D.; Skoulios, A.; Dexpert, H.; Giroud-Godguin, A. M.; Marchon, J. C. *J. Phys. (France)* **1988**, *49*, 345–352.
- (2) Serrete, A.; Carroll, P. J.; Swager, T. M. *J. Am. Chem. Soc.* **1992**, *114*, 1887–1889.
- (3) Trzaska, S. T.; Swager, T. M. *Chem. Mater.* **1998**, *10*, 438–443.
- (4) Szydłowska, J.; Pyżuk, W.; Krówczyński, A.; Bikchantsev, I. *J. Mater. Chem.* **1996**, *6*, 733–738.
- (5) Krówczyński, A.; Szydłowska, J.; Pocięcha, D.; Przedmojski, J.; Górecka, E. *Liq. Cryst.* **1998**, *25*, 117–121.
- (6) Krówczyński, A.; Szydłowska, J.; Górecka, E. *Liq. Cryst.* **1999**, *26*, 685–689.
- (7) Lai, C. K.; Pang, Yung-Shen; Tsai, Chun-Hsien. *Liq. Cryst.* **1998**, *8*, 2605–2610.
- (8) Lai, C. K.; Lu, Min-Yi; Lin, Fun-Jane. *Liq. Cryst.* **1997**, *23*, 313–315.

Scheme 2



Scheme 3



evaporated overnight, and crude product (4) was chromatographed on silica gel eluted with hexane/methylene chloride solvent (2:1). Yield, ~80%.

For [1,2-di(2'-octyl-3'-oxo-1'-dodecylamino)-4-acetylbenzo]nickel(II). $^1\text{H NMR}$ (CDCl_3): δ 0.88–0.92 (m, 12H, $(\text{CH}_2)_7\text{CH}_3$ and $(\text{CH}_2)_8\text{CH}_3$), 1.20–1.70 (m, 52H, $\text{CH}_2(\text{CH}_2)_6\text{CH}_3$ and $\text{CH}_2(\text{CH}_2)_7\text{CH}_3$), 2.32–2.37 (m, 4H, $\text{C}=\text{CCH}_2$), 2.44–2.50 (m, 4H, COCH_2), 2.60 (s, 3H, COCH_3), 7.42–7.57 (m, 4H, $\text{H}_1^{5,6}$ and NCH), 8.09 (d, $J = 1.5$ Hz, H, H^3).

2.1.2. Sodium Salt of [1,2-Di(2'-octyl-3'-oxo-1'-dodecylamino)-4-(3''-oxo-1''-propionyl)benzo]metal(II) (4). Complex 3 (1 mmol) suspended in ether (100 cm^3) and ethyl formate (2.2 mmol) was introduced into molecular sodium (1.1 mmol) covered with ether. The reaction mixture was left for 12 h, and then ether was evaporated under vacuum. The remaining precipitate containing mainly nonpurified 4 was used in the next reaction step.

2.1.3. The Binuclear Complexes (1). 1,2-Dioctyloxy-4-[3'-oxo-3''-(2'',3'',4''-trioctyloxyphenyl)-1'-propenylamino]-5-aminobenzen⁵ (1 mmol) and the sodium salt 4 (ca. 1.1 mmol) were suspended in 2-butoxyethanol (50 cm^3), neutralized with acetic acid, and kept at 90 °C for 10 min.

To obtain a tetradentate nonpurified ligand, a methanol solution (50 cm^3) of the appropriate metal salt, $(\text{Ni}(\text{OAc})_2)$, $\text{Cu}(\text{OAc})_2$, or $\text{VO}(\text{acac})_2$ (1.1 mmol), was introduced. The mixture was heated for 5 min and then cooled to room temperature. Tarry precipitate of complex 1 was filtered off and recrystallized from 2-propanol. The pure complex was obtained from thin-layer chromatography on silica gel eluted with hexane/methylene chloride solvent (1:2). Yield, ~30–40%.

For binuclear complexes $1 = \text{L}^1\text{MM}'$. L^1Ni_2 . $^1\text{H NMR}$ (CDCl_3): δ 0.82–0.94 (m, 27H, CH_3), 1.18–1.88 (m, 112H, $\text{CH}_2(\text{CH}_2)_6\text{CH}_3$ and $\text{CH}_2(\text{CH}_2)_7\text{CH}_3$), 2.25–2.37 (m, 4H, $\text{C}=\text{CCH}_2$), 2.41–2.50 (m, 4H, COCH_2), 3.93–4.03 (m, 10H, OCH_2), 6.18 (d, $J = 6.3$ Hz, H, NCHCH), 6.70 and 7.61 (AB system, $J = 8.8$ Hz, 2H, C_6H_2), 6.99 and 7.01 (2s, 2H, C_6H_2), 7.38–7.56 (m, 6H, two protons from C_6H_3 , NCHCH , NCH), 8.02 (broad s, H, one proton from C_6H_3). $^{13}\text{C NMR}$ (CDCl_3): δ 14.125, 22.695, 22.72, 26.07, 26.13, 26.17, 26.21, 26.33, 26.46, 29.30, 29.33, 29.40, 29.52, 29.58, 30.46, 31.85, 31.91, 31.96, 68.61, 70.02, 73.73, 74.62, 95.09, 99.01, 108.03, 108.96, 109.80, 111.56, 112.12, 122.39, 125.05, 131.83, 136.00, 136.49, 141.87, 142.68, 144.84, 145.99, 146.15, 146.98, 146.19, 148.06, 148.47, 152.01, 155.10, 172.85, 173.35, 184.32, 185.58. Anal. Calcd for $\text{C}_{104}\text{H}_{170}\text{N}_4\text{Ni}_2\text{O}_9$ (1737.9): C, 71.87; H, 9.86; N, 3.22. Found: C, 71.77; H, 9.92; N, 3.15. IR (CH_2Cl_2 , ν , cm^{-1}): 2958, 2926, 2855 (C–H str), 1601–1562 (C=O, C=C–N str), 1327 (Ar–N str), 1266 (ArO–C str). UV–vis (CH_2Cl_2 , λ , nm): 234, 306, 428, 448, 509.

For L^1Cu_2 . Anal. Calcd for $\text{C}_{104}\text{H}_{170}\text{N}_4\text{Cu}_2\text{O}_9$ (1747.62): C, 71.42; H, 9.81; N, 3.21. Found: C, 71.67; H, 9.92; N, 3.19. IR (CH_2Cl_2 , ν , cm^{-1}): 2956, 2930, 2855 (C–H str), 1606–1565 (C=O, C=C–N str), 1322 (Ar–N str), 1264 (ArO–C str). UV–vis (CH_2Cl_2 , λ , nm): 229, 263, 391, 434, 460, 516.

For L^1NiCu . Anal. Calcd for: $\text{C}_{104}\text{H}_{170}\text{N}_4\text{CuNiO}_9$ (1742.76): C, 71.87; H, 9.83; N, 3.21. Found: C, 71.67; H, 9.92; N, 3.25. IR (CH_2Cl_2 , ν , cm^{-1}): 2956, 2927, 2856 (C–H str), 1602–1562 (C=O, C=C–N str), 1327 (Ar–N str), 1264 (ArO–C str). UV–vis (CH_2Cl_2 , λ , nm): 229, 298, 385, 418, 458, 512. MS (ESI in MeOH + 1% AcOH): m/z 1741 [$\text{M} + \text{H}^+$], 1763 [$\text{M} + \text{Na}^+$].

For L^1CuNi . Anal. Calcd for $\text{C}_{104}\text{H}_{170}\text{N}_4\text{CuNiO}_9$ (1742.76): C, 71.87; H, 9.83; N, 3.21. Found: C, 71.98; H, 9.97; N, 3.20. IR (CH_2Cl_2 , ν , cm^{-1}): 2956, 2927, 2856 (C–H str), 1602–1562 (C=O, C=C–N str), 1327 (Ar–N str), 1264 (ArO–C str). UV–vis (CH_2Cl_2 , λ , nm): 229, 312, 381, 431, 452, 514. MS (ESI in MeOH + 1% AcOH): m/z 1741 [$\text{M} + \text{H}^+$], 1763 [$\text{M} + \text{Na}^+$].

For $\text{L}^1(\text{VO})_2$. Anal. Calcd for $\text{C}_{104}\text{H}_{170}\text{N}_4(\text{VO})_2\text{O}_9$ (1754.41): C, 71.20; H, 9.77; N, 3.19. Found: C, 70.96; H, 9.64; N, 3.05. IR (CH_2Cl_2 , ν , cm^{-1}): 2957, 2928, 2856 (C–H str), 1601–1558 (C=O, C=C–N str), 1320 (Ar–N str), 1272 (ArO–C str), 989 (V=O str). MS (ESI in MeOH + 1% AcOH): m/z 1754 [$\text{M} + \text{H}^+$], 1776 [$\text{M} + \text{Na}^+$].

For $\text{L}^1\text{Cu}(\text{VO})$. Anal. Calcd for $\text{C}_{104}\text{H}_{170}\text{N}_4\text{Cu}(\text{VO})\text{O}_9$ (1751.01): C, 71.33; H, 9.79; N, 3.20. Found: C, 71.18; H, 9.90; N, 3.14. IR (CH_2Cl_2 , ν , cm^{-1}): 2956, 2929, 2856 (C–H str), 1579–1554 (C=O, C=C–N str), 1316 (Ar–N str), 1270 (ArO–C str), 980 (V=O str). UV–vis (CH_2Cl_2 , λ , nm): 227, 264, 392, 449, 470.

For $\text{L}^1\text{Ni}(\text{VO})$. Anal. Calcd for $\text{C}_{104}\text{H}_{170}\text{N}_4\text{Ni}(\text{VO})\text{O}_9$ (1746.15): C, 71.53; H, 9.81; N, 3.21. Found: C, 71.28; H, 9.96; N, 3.09. IR (CH_2Cl_2 , ν , cm^{-1}): 2956, 2928, 2856 (C–H str), 1601–1559 (C=O, C=C–N str), 1322 (Ar–N str), 1264 (ArO–C str), 987 (V=O str).

2.1.4. The Trinuclear Complexes (2). The syntheses of the trinuclear complexes (2) were similar to the syntheses of the binuclear complexes (1). 1,2-Dioctyloxy-4,5-diaminobenzene (1 mmol) and the sodium salt 4 (ca. 2.2 mmol) were suspended in 2-butoxyethanol (50 cm^3), neutralized with acetic acid, and heated. To the resulting crude ligand, a methanol solution (50 cm^3) of appropriate metal salt ($(\text{Ni}(\text{OAc})_2)$, $\text{Cu}(\text{OAc})_2$, or $\text{VO}(\text{acac})_2$) (1.1 mmol) was added. After the mixture was heated and then cooled, the solid precipitate of complex 2 was filtered off and recrystallized from 2-propanol. The purification of 2 was performed with thin-layer chromatography. Yield, ~50%.

For trinuclear complexes $2 = \text{L}^2\text{M}_2\text{M}'$. L^2Ni_3 . $^1\text{H NMR}$ (CDCl_3): δ 0.82–0.93 (m, 30H, CH_3), 1.14–1.86 (m, 128H, $\text{CH}_2(\text{CH}_2)_6\text{CH}_3$ and $\text{CH}_2(\text{CH}_2)_7\text{CH}_3$), 2.24–2.37 (m, 8H, $\text{C}=\text{CCH}_2$), 2.40–2.51 (m, 8H, COCH_2), 3.97 (t, $J = 6.6$ Hz, 4H, OCH_2), 6.18 (d, $J = 6.3$ Hz, 2H, NCHCH), 6.97 (s, 2H, C_6H_2), 7.38–7.58 (m, 10H, NCHCH , two protons from C_6H_3 , NCH), 8.02 (broad s, 2H, one proton from C_6H_3).

Table 1. Liquid Crystalline Phases, Phase Transition Temperatures (in °C), and Phase Transition Enthalpy Changes (in Parentheses, J g⁻¹) for the Synthesized Complexes

complexes 1			complexes 2		
M	M'		M	M'	
Ni	Ni	D_{hd} , 100.7 (1.8), I	Ni	Ni	D_{rd} , 106; ^a D_{hd} , 162.2 (1.1), I
Cu	Cu	D_{hd} , 137.3 (2.0), I	Cu	Cu	D_{rd} , 124; ^a D_{hd} , 197.1 (1.1), I
Ni	Cu	D_{hd} , 125.3 (1.5), I	Ni	Cu	D_{rd} , 100; ^a D_{hd} , 161.3 (2.2), I
Cu	Ni	D_{hd} , 117.3 (1.5), I	Cu	Ni	D_{rd} , 130; ^a D_{hd} , 190.1 (1.3), I
VO	VO (α)	D_{hd} ~80, ^a I	Ni	VO	D_{hd} , 162–163, ^a I
VO	VO (β)	D_{hd} ~120, ^a I	Cu	VO	D_{hd} , 172–178, ^a I
Cu	VO	D_{hd} , 155.4 (2.7), I			
Ni	VO	D_{hd} , 147.4 (1.4), I			

^a From microscopy.

¹³C NMR (CDCl₃): δ 14.14, 14.18, 22.71, 22.74, 26.08, 26.32, 26.36, 29.33, 29.38, 29.42, 29.45, 29.49, 29.56, 29.59, 29.64, 29.69, 29.78, 29.81, 31.48, 31.64, 31.87, 31.92, 31.95, 31.98, 32.00, 32.80, 32.85, 35.67, 35.91, 69.96, 95.23, 98.97, 109.18, 109.82, 110.66, 111.24, 112.27, 122.27, 131.70, 136.20, 142.67, 144.86, 146.06, 147.10, 147.89, 143.24, 184.29, 185.50. Anal. Calcd for C₁₂₀H₁₉₄N₆Ni₃O₈ (2024.98): C, 71.17; H, 9.66; N, 4.15. Found: C, 71.30; H, 9.73; N, 4.08. IR (CH₂Cl₂, ν , cm⁻¹): 2957, 2927, 2854 (C–H str), 1594–1564 (C=O, C=C–N str), 1330 (Ar–N str), 1264 (ArO–C str). UV–vis (CH₂Cl₂, λ , nm): 238, 304, 415, 449, 471, 561.

For L²Cu₃. Anal. Calcd for C₁₂₀H₁₉₄N₆Cu₃O₈ (2039.54): C, 70.66; H, 9.59; N, 4.12. Found: C, 71.01; H, 9.70; N, 4.05. IR (CH₂Cl₂, ν , cm⁻¹): 2954, 2927, 2857 (C–H str), 1600–1566 (C=O, C=C–N str), 1333 (Ar–N str), 1264 (ArO–C str). UV–vis (CH₂Cl₂, λ , nm): 229, 263, 392, 453, 476.

For L²Ni₂Cu. Anal. Calcd for C₁₂₀H₁₉₄N₆CuNi₂O₈ (2029.83): C, 71.00; H, 9.63; N, 4.14. Found: C, 71.08; H, 9.72; N, 4.06. IR (CH₂Cl₂, ν , cm⁻¹): 2956, 2927, 2854 (C–H str), 1590–1564 (C=O, C=C–N str), 1329 (Ar–N str), 1266 (ArO–C str). UV–vis (CH₂Cl₂, λ , nm): 237, 300, 419, 450, 481. MS (ESI in MeOH + 1% AcOH): m/z 2026 [M⁺].

For L²Cu₂Ni. Anal. Calcd for C₁₂₀H₁₉₄N₆Cu₂NiO₈ (2034.69): C, 70.83; H, 9.61; N, 4.13. Found: C, 71.00; H, 9.58; N, 4.20. UV–vis (CH₂Cl₂, λ , nm): 232, 304, 379, 451, 468.

For L²Ni₂(VO). Anal. Calcd for C₁₂₀H₁₉₄N₆Ni₂(VO)O₈ (2033.23): C, 70.88; H, 9.62; N, 4.13. Found: C, 71.06; H, 9.68; N, 4.20. IR (CH₂Cl₂, ν , cm⁻¹): 2957, 2927, 2855 (C–H str), 1594–1560 (C=O, C=C–N str), 1328 (Ar–N str), 1265 (ArO–C str), 988 (V=O str). UV–vis (CH₂Cl₂, λ , nm): 237, 301, 416, 450, 495.

For L²Cu₂(VO). Anal. Calcd for C₁₂₀H₁₉₄N₆Cu₂(VO)O₈ (2042.94): C, 70.55; H, 9.57; N, 4.11. Found: C, 70.49; H, 9.45; N, 4.08.

2.2. Measurements. The mesophase identification was based on routine microscopic examination of textures. A Zeiss Jenapol-U polarizing microscope equipped with a Mettler FP82HT hot stage was used. For some compounds the designation of the mesophase structure was supported by X-ray studies using a DRON spectrometer. Phase transition temperatures were mainly determined by calorimetric measurements performed with a Perkin-Elmer DSC-7. When heat effects were undetectable, the temperatures of phase transitions were taken from microscopic observation. ESR investigations were performed in the X-band on a Radiopan spectrometer equipped with a nitrogen flow heater. The resulting spectra were analyzed by Bruker's software package Symphonia. NMR spectra were recorded by a Varian Unity Plus spectrometer operating at 500 MHz, and IR spectra were obtained with a Nicolet Magna IR 500 spectrometer. Molecular dimensions were estimated by molecular modeling (HYPERCHEM).

3. Results and Discussion

3.1. Phase Sequence and X-ray Studies. The synthesized series of complexes **1** and **2** have disk-shaped molecules and form columnar phases that are stable at room temperature. Phase sequence and phase transition temperatures for the compounds studied are collected in Table 1.

Table 2. X-ray Signals Corresponding to Crystallographic Distances (in Å), Calculated Dimensions of the Crystallographic Cell, and Estimated Density (g cm⁻³)

phase	M	M'	Bragg signal		diffused signal	cell dimensions	density
			(110) = (200)				
Complex 1							
D_{hd}	Cu	Cu	24.12	4.392		48.2 × 27.9 × 4.4	0.96
D_{hd}	Cu	Ni	24.12	4.486		48.2 × 27.9 × 4.5	0.96
phase	M	M'	Bragg signal		diffused signal	cell dimensions	density
			110	200			
Complex 2							
D_{hd}	Ni	Ni	24.85	24.85	4.5	49.7 × 28.1 × 4.5	1.07
D_{rd}	Ni	Ni	24.48	28.7	4.2	57.4 × 27.1 × 4.2	1.03

For binuclear compounds **1**, only the disordered hexagonal columnar phase was found. The compounds form a smooth pseudo-fan-like texture with sharp boundaries between domains.⁹ At clearing points the transition enthalpy is rather small, and for the vanadyl–vanadyl complex this enthalpy was not observed. The bivanadyl substance due to low symmetry of the chelating centers (C₁)⁶ actually consists of two diastereoisomeric forms, α and β , which for the most plausible conformation (shown in the Scheme 2) have the oxygen atoms attached to the same or the opposite side of the coordination planes. Using thin layer (nonchiral) chromatography, we were able to separate these diastereoisomers probably because of their different polarities or dissimilarity of their shapes. For the separated substances the clearing temperatures greatly differ (about 40 °C). The α and β diastereoisomers are stable at room temperature; however, when kept for several minutes at an elevated temperature close to the clearing points, they isomerize to give a mixture of both diastereoisomers. This process can also result from possible exchange of metals in metallic centers at elevated temperatures.

The microscopically identified disordered hexagonal columnar phase seems to be confirmed by X-ray studies (Table 2). On diffractograms of the binuclear complexes only one very strong signal is observed, which was assigned to the strongest (110) = (1 -1 0) = (200) reflection. The complexes investigated have similar crystalline lattices, and the lattice periodicity was nearly temperature-independent. The calculated dimensions of crystallographic cells suggest that in the D_{hd} phase the molecules in their most extended conformations should interdigitate three to four carbon atoms of the alkyl chains.

The complexes of trinuclear series **2** just below the isotropic phase reveal the hexagonal disordered columnar phase. At lower temperatures they form the disordered rectangular columnar phase except for the vanadyl complexes, which exhibit the hexagonal phase only. The transition to the rectangular columnar phase is accompanied by appearance of a broken pseudo-fan texture observed in microscopy. At the transition points between the columnar phases the transition enthalpy is not detected.

The X-ray studies of the series of complexes **2** seem to confirm the identified columnar phases. For the Ni–Ni–Ni complex the lower temperature phase gives two Bragg signals, which match only to a rectangular structure. The strongest one was probably related to the (110) = (1 -1 0) reflections. For the molecules with the most extended conformation of the terminal chains, the appearance of the rectangular lattice of the determined size requires interdigitated packing of the outside chains to three or four carbon atoms in depth.

(9) Destrade, C.; Foucher, P.; Gasparou, H.; Tinh, N. H.; Levelut, A. M.; Malthete, J. *Mol. Cryst. Liq. Cryst.* **1984**, *106*, 121–146.

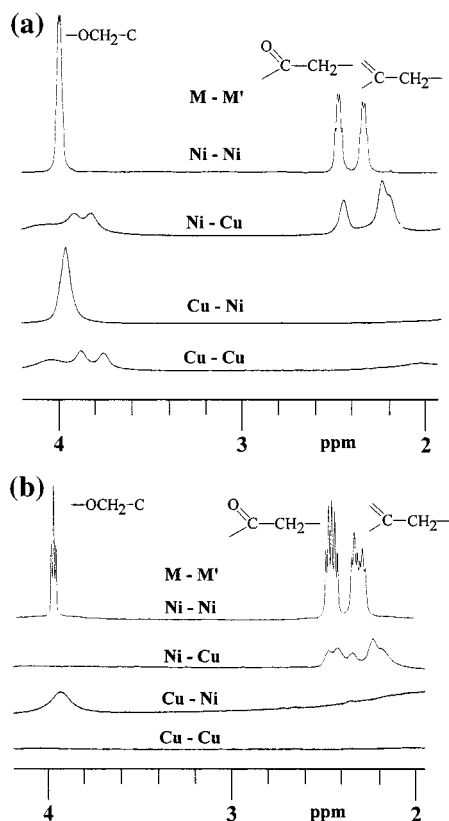


Figure 1. ^1H NMR spectra of the series of (a) complexes **1** and (b) complexes **2**.

3.2. NMR Studies. The influence of the paramagnetic copper ion on the proton in methylene ($-\text{CH}_2-$) moieties was reflected by the NMR spectra of the bi- and trinuclear nickel and copper complexes (parts a and b of Figure 1, respectively). The NMR signals of methylene groups that are situated at the paramagnetic copper center are so strongly broadened that they are not even observed. When methylene groups are at the nonparamagnetic nickel center and when simultaneously the next center is paramagnetic, then the NMR signal is strongly influenced. For the copper–nickel, copper–copper, copper–nickel–copper, and copper–copper–copper complexes the NMR signals of the methylene groups $=\text{C}(\text{CH}_2)-$ and $\text{O}=\text{C}(\text{CH}_2)-$ are not detected. The signals for nickel–copper and nickel–copper–nickel complexes are strongly affected.

A similar broadening and a slight shifting of the signal are observed for the $-\text{O}-\text{CH}_2-$ protons introduced into the trinuclear copper–nickel–copper complex and substituted at the phenyl ring near the nonparamagnetic nickel center. The distance for this copper–proton interaction measured along the bonding in para positions of the outer phenyl and enaminoketone rings is about 15 \AA . The related $-\text{O}-\text{CH}_2-$ signal coming from the binuclear copper–nickel complex seems to be less broadened. This signal is given by protons of the alkoxy groups substituted at two places of the molecule: at the *o*-diaminophenyl moiety, which is identical to that for trinuclear complexes, and at the phenylcarbonyl moiety introduced only into the binuclear complexes. The superposition of the signals of these two groups results in a sharper peak probably because the protons of the three alkoxy groups attached to the phenyl ring are almost not influenced by paramagnetic copper ion, which is situated at the outer M position (Scheme 2). In this case the interaction path length measured along the molecular bonding with $-\text{N}-\text{phenyl}-\text{N}-$ was estimated to be 22 \AA ,

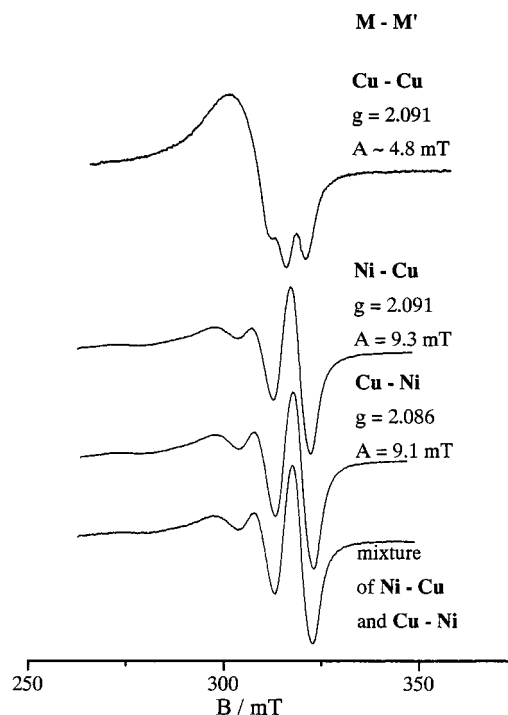


Figure 2. ESR spectra of the copper complexes (**1**) in methylene chloride solution at $\sim 40 \text{ }^\circ\text{C}$.

which is much larger than for two $-\text{O}-\text{CH}_2-$ protons substituted at the *o*-diaminophenyl ring. It indicates that the unpaired spin of hydrogen atoms could be affected by the unpaired spin of a metallic ion placed not farther than at next-nearest chelating unit. However, it should be pointed out that the interaction of the magnetic dipoles does not only depend on the linear distance between the interacting entities.¹⁰

3.3. ESR Studies. The interaction of unpaired spins belonging to paramagnetic centers was studied by the ESR method. The series of compounds of **1** with the single paramagnetic copper ion dissolved in methylene chloride solution exhibit the usual isotropic spectra with four hyperfine features (Figure 2). In these spectra the electron exchange coupling between the paramagnetic entities is not observed. The ESR spectrum of a binary mixture of two binuclear complexes having a single copper ion at different position (M or $\text{M}' = \text{Cu}$) in methylene chloride solvent does not reveal such interaction either. However, for the bicopper compound (M and $\text{M}' = \text{Cu}$) under the same conditions the hyperfine structure of the spectrum is doubled; the separation of the hyperfine signals is 2 times smaller than that for the compounds with a single copper ion. This unambiguously shows that two copper ions built into the same molecule are close enough to form a coupled system.¹¹ In this case the spin superexchange interaction is transmitted through an approximated 10 \AA distance probably by the π bonding system joining two metallic centers.^{12,13}

Better separation of the hyperfine signals was observed for a temperature close to the boiling point of the solvent, about 40

(10) Eaton, D. R. In *NMR of Paramagnetic Molecules*; La Mar, G. N., Horrocks, W. DeW., Jr., Holm, R. H., Eds.; Academic Press: New York, 1973.

(11) Weil, J. W.; Bolton, J. R.; Wertz, J. E. *Electron Paramagnetic Resonance; Elementary Theory and Practical Applications*; John Wiley and Sons: New York, 1994.

(12) Hatfield, W. E. In *Theory and Applications of Molecular Paramagnetism*; Boudreaux, E. A., Mulay, L. N., Eds.; John Wiley and Sons: New York, 1976.

(13) Inoue, M. B.; Velazquez, E. F.; Medrano, F.; Ochoa, K. L.; Galvez, J. C.; Inoue, M.; Fernando, Q. *Inorg. Chem.* **1998**, *37*, 4070–4075.

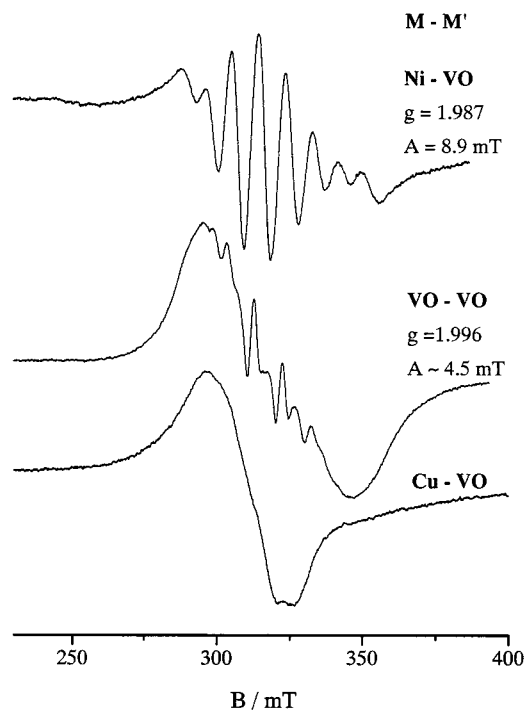


Figure 3. ESR spectra of the vanadyl complexes of **1** in methylene chloride solution.

°C. At room temperature the hyperfine structure is blurred by the one unresolved signal coming plausibly from exchange narrowing, which is stronger at lower temperatures owing to slower molecular motions. The solution frozen in liquid nitrogen gave only one broad ESR signal, which probably resulted from precipitation of the complex.

An analogous electron exchange interaction seems to be observed for the vanadyl–vanadyl complex in methylene chloride solution (Figure 3). The ESR isotropic spectrum exhibits hyperfine structure with hyperfine spacing, which is half the value determined for the monovanadyl complex. The doubled hyperfine spectra of bivanadyl compounds are rather rare; however, it has been already described for some tartrate complexes.¹⁴ The nickel–vanadyl complex solution reveals eight hyperfine signals that confirm the absence of the intermolecular exchange coupling of the oxovanadium groups. For the ESR spectrum of the binuclear complex with two paramagnetic centers, copper and vanadyl, a broad noninformative signal was registered that reflects the strong spin–spin narrowing interaction.

The intramolecular coupling of two unpaired electrons results in an electron triplet state. For coupled electrons with total spin $S = 1$ apart from the signal $\Delta M_s = \pm 1$, a small signal of the forbidden transition $\Delta M_s = \pm 2$ can be observed. For the copper–copper complex this transition was detected in the liquid crystalline phase. For the half-field region the EPR spectrum reveals a broad, faint peak that confirms the formation of the triplet state (Figure 4). At the usual high-field range a broad signal of the $\Delta M_s = \pm 1$ transition appears, but it is much stronger. In both cases, low and high field, the EPR signals characteristic of the copper–copper complex are brought together by the exchange-narrowing process, which is very frequent for magnetically concentrated substances.

The trinuclear complex **2** with two copper ions substituted in outer, not-neighboring centers ($M = \text{Cu}$, $M' = \text{Ni}$) gives in

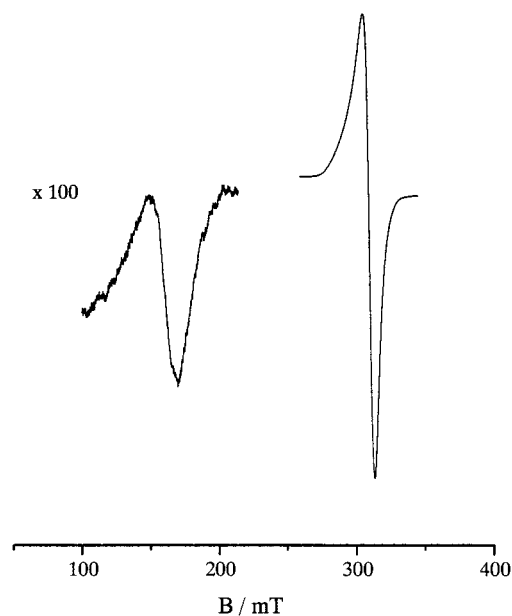


Figure 4. ESR spectrum of the copper–copper complex **1** for the D_{hd} phase.

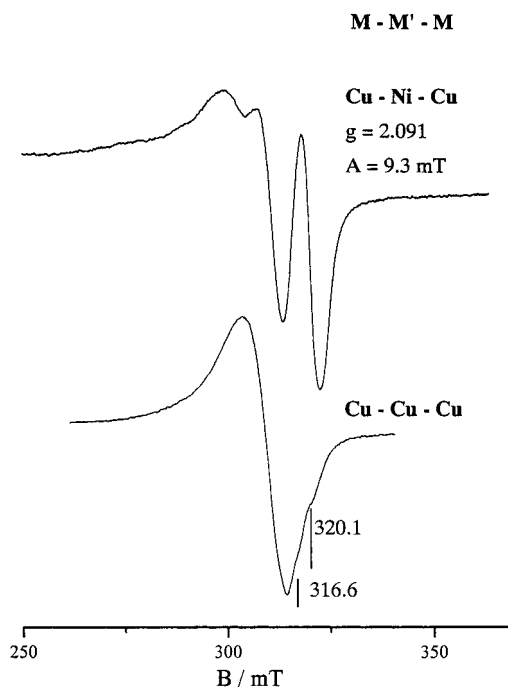


Figure 5. ESR spectra of the copper complexes **2** in methylene chloride solution at ~ 40 °C.

solution an ESR spectrum typical of separated paramagnetic entities (Figure 5). It excludes the electron spin interaction and indicates that the electron exchange coupling cannot be transmitted through free space at a distance of 15 Å. When three copper ions occupy metallic centers, the hyperfine peaks for methylene chloride solution are blurred owing to the exchange narrowing. However, slight signals can be seen that exhibit the doubled hyperfine structure coming from electron exchange coupling between pairs of neighboring copper ions.

For the nickel–vanadyl complex of the series (**1**) the exchange-narrowing processes are less effective and resolved ESR spectra can be observed. In the hexagonal disordered columnar phase the ESR spectrum is typical of the vanadium-(IV) ion in uniaxial configuration (Figure 6). At temperatures

(14) Belford, R. L.; Chasten, N. D.; So, H.; Tapscott, R. E. *J. Am. Chem. Soc.* **1969**, *91*, 4675–4680.

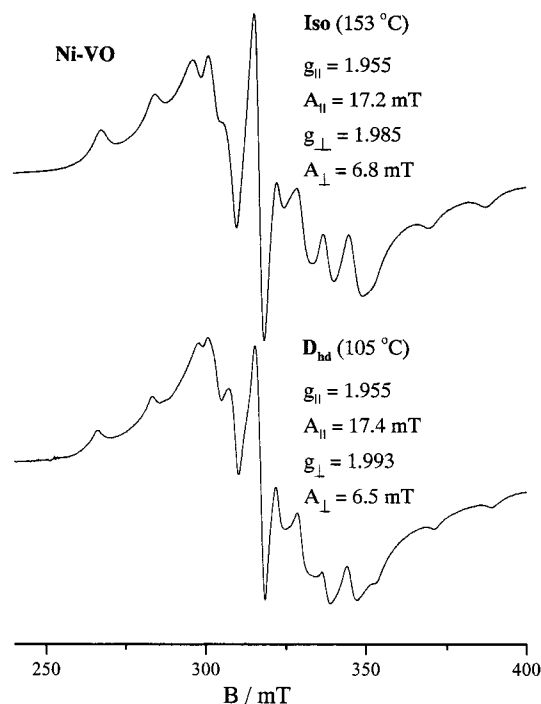


Figure 6. ESR spectra of the nickel–vanadyl complex **1** for the isotropic and D_{hd} phases.

above the isotropisation point the spectrum remains almost unchanged and molecular uniaxiality is preserved. It could be explained by supposition that in the isotropic phase the restriction of molecular rotation is not fully removed and molecules rotate much more easily around one axis than around two others. This effect is common especially for high-viscosity liquids, and on the ESR time scale the uniaxial phase can be observed. Moreover, the microscopically detected isotropic phase can actually be formed from some anisotropic area, smaller than the wavelength of visible light. The similar maintenance of the anisotropic properties in the isotropic phase has been already found for the vanadyl ions in ESR studies.¹⁵

4. Conclusions

The described bi- and trinuclear tetradentate *cis*-enaminoketone complexes with various combinations of metallic centers due to their disklike molecular shapes reveal liquid crystalline D_{hd} and D_{rd} columnar phases that are stable over a broad temperature range. The distinctly higher clearing temperature found for the square-pyramidal vanadoxy complexes compared with the relevant complexes with planar geometry could suggest mesophase stabilization by an intracolumnar linear chain structure formed by $\cdots V=O\cdots V=O\cdots$ interaction.^{2,16} The long distance molecular head to tail organization of $V=O$ moieties could result in the columnar ferroelectricity. However, for the copper–vanadyl and the vanadyl–vanadyl complexes, ferroelectric switching was not observed; no traces of current peaks under application of an ac electric field were found. Moreover, IR studies of the binuclear copper–vanadyl complex exclude the intracolumnar vanadyl–vanadyl interaction. The IR signals related to the $V=O$ bond stretching recorded for solid, liquid crystalline film, and dichloromethane solution were found at the positions $\nu_{V=O} = 982$, $\nu_{V=O} = 980$, and $\nu_{V=O} = 988$ cm^{-1} ,

respectively. They are very similar and correspond to the separated $V=O$ bonding.¹⁶ Also, the formation of two diastereoisomers of the vanadyl–vanadyl complexes that are stable at room temperature excludes the frequent switching of the oxygen atom between neighboring vanadium ions in the chain structure. However, the separated diastereoisomers of the vanadyl–vanadyl complex do not preserve their properties at elevated temperature; thus, the bonding of the oxygen atom at the vanadoxy centers is not strong enough to encourage the stable chiral properties of these low-symmetry molecules. This suggests weak mobility of the oxygen atom within the column of the liquid crystalline phase. Also, the ESR investigation suggests that the vanadyl complexes form monomeric phase structure. The ESR spectrum registered for the nickel–vanadyl complex in columnar phase is typical of the separated VO^{2+} paramagnetic entity.

The unpaired electron of the paramagnetic metallic ion influences the magnetic moments of quite distant (15 Å) protons in the molecule. This interaction is allowed because of the presence of delocalized unpaired spin distributed over the molecule. The vast range of interaction suggests that the spin density is delocalized in the conjugated π bonding system because the direct mechanism of the unpaired spin transfer into a σ molecular orbital leads to a rapid spin attenuation in a few bonds.¹⁰ The $-N-C$ bond system can be considered as conjugative because of the free electron pair localized on the nitrogen atom. The direct connection of the nitrogen atom to the aromatic moieties and the planar structure of the chelating center probably allow the extension of the conjugated π bonds over the whole enaminoketone unit and the propagation of spin density. The transmission of the spin density to the other chelating unit is somewhat inhibited owing to the presence of a nonconjugative $-C=O-$ moiety on the path that links two metallic centers. However, this attenuation is not total and the influence of the copper ion on the methyl groups of the dialkoxyphenyl moiety (which is 15 Å distant) was detected. For the trialkoxyphenyl moiety, which is more distant, the spin transmission to the methyl groups is significantly weaker and only the meaningless interaction between proton and copper ion was observed. In this case the π bonding system that could propagate unpaired spin includes two nonconjugative $-(C=O)-$ groups. Moreover, the *cis* configuration of *o*-diaminophenylene moiety, which is supposed to be the spin-transfer path, might be less effective as the conjugative π system because of its substantial bending.

The superexchange coupling between metallic centers of the binuclear complexes found in the ESR studies reflects the weak interaction between the electrons of the paramagnetic entities. The detected range of the superexchange interaction is similar to that observed in the NMR study for the copper ion and protons. The relatively long distance of copper–copper and vanadyl–vanadyl exchange coupling suggests that it operates through conjugated π electron bondings. The coupling between unpaired electrons of copper ions when the interaction should be transmitted at a distance of 15 Å through free space is not observed.

The electron coupling ground state with paired or unpaired spins results in magnetic properties of the investigated copper–copper and vanadyl–vanadyl complexes. For the lower lying triplet state the ferromagnetic interaction is present, whereas for the antiferromagnetic interaction the ground state is the singlet state. However, even for the antiferromagnetic-type interaction the higher energy triplet state can be thermally

(15) Alonso, P. A. *Metallomesogens: Synthesis, Properties, and Applications*; Serrano, J. L., Ed.; VCH Publishers, Inc.: Weinheim, 1996.
 (16) Serrete, A. G.; Swager, T. M. *J. Am. Chem. Soc.* **1993**, *115*, 8879–8880.

populated and paramagnetic properties can be observed in ESR studies. To determine whether the investigated compounds are ferro- or antiferromagnetic, further studies of magnetic susceptibility are necessary.

Acknowledgment. KBN Grant 3T09A04615 is greatly acknowledged.

IC0000808